

DETECTING SAHARAN DUST STORMS USING SEAWIFS IMAGERY

*K. L. Carder, F. R. Chen, C. Catrall, and A. A. Strub
University of South Florida
Department of Marine Science
140 – 7th Avenue South
Saint Petersburg, FL 33701*

ABSTRACT

Aerosol iron is believed to be an important micro-nutrient for phytoplankton growth in waters replete in nitrogen or rich in nitrogen-fixing bacteria. Since iron-rich dust absorbs radiation at the blue end of the visible spectrum, if the contribution made by water-leaving radiance from the ocean is known, satellite sensors such as SeaWiFS and MODIS can spectroscopically detect its presence. A significant input of Saharan dust was visually detected over the Bahamas from an airplane and from the ground in late May 1998. TOMS satellite imagery helped to pinpoint the location of a likely dust cloud for that period over the clear waters of the Sargasso Sea, and SeaWiFS imagery was examined to ascertain spectral characteristics consistent with an increase in aerosol absorption with decreasing wavelength. This behavior was compared to absorption effects expected using literature absorption spectra for Saharan dust. Derivation of aerosol radiance spectra for green and red SeaWiFS wavelengths was carried out in a manner similar to CZCS methods for clear waters, and an explanation provided for low-chlorophyll anomalies that covaried with blue-absorbing dust and high-altitude aerosol locations. A method of flagging likely dust-rich pixels is presented.

INTRODUCTION

Recent suggestions that iron concentrations may limit phytoplankton growth in oligotrophic waters (Martin and Fitzwater 1988) have led to several iron-enrichment investigations. Surges in plant productivity, chlorophyll pigment concentration, and biomass were observed after a major iron enrichment of 64 km² in the equatorial Pacific (Martin, Coale et al. 1994), and in waters near Hawai'i during a major pulse of iron-rich dust from Asia (Young, Carder et al. 1991). The latter study showed that a mere 10% iron dissolution of the aerosol particles while sinking through the water column would explain the observed systematic increases of plant production with depth and time. These results suggest that iron-bearing aerosols may be an important source of iron to plants in the oligotrophic ocean regions.

Desert dust such as that from the Saharan or Gobi deserts, however, often contain iron in oxide form which can cause distinct color variations, or spectral absorption. In fact, iron is the element most responsible for the color of dust (Hurst 1977; Patterson 1981). Saharan dust, for example, often absorbs far more strongly in the blue wavelengths than the yellow and red (Lindberg and Laude 1974; Patterson 1981), resulting in a reddish-brown aerosol. Saharan dust is swept in vast quantities into the air streams over the west African coast in the dry summer months, and transported thousands of miles across the Atlantic Ocean to the Caribbean and eastern United States (Schutz, Jaenicke et al. 1981).

This provides incorrect determinations of the water-leaving radiance (Carder, Hawes et al. 1991). Accurate determination of the water-leaving radiance in the blue portion of the spectrum is of crucial importance in determining the chlorophyll pigment concentration and primary production within oceanic environments.

PHYSICS OF THE PROBLEM

Radiance resulting from scattering is denoted in the literature by $L_x(\lambda)$, where x represents the source of the scattered signal, such as Rayleigh (R), aerosol (a), or multiple (ar, ra) scattering. It is more convenient and physically meaningful to use *reflectance* (Gordon and Clark 1981) (θ_o representing the solar zenith angle and F_o the extraterrestrial solar irradiance),

$$\rho_x(\lambda) = \frac{\pi}{F_o(\lambda) \cdot \cos\theta_o} L_x(\lambda).$$

The complete formulation of the correction algorithms have been thoroughly documented (Gordon and Clark 1981; Gordon, Brown et al. 1988; Gordon and Wang 1994) and shall not be reviewed here. The quantity of importance is the ratio of single-scattering aerosol reflectances (denoted by subscript *as*) received by the sensor at wavelengths λ_i and λ_j and a viewing angle θ_v :

$$\varepsilon(\lambda_i, \lambda_j) \equiv \frac{\rho_{as}(\lambda_i)}{\rho_{as}(\lambda_j)} = \frac{\omega_a(\lambda_i) \cdot \tau_a(\lambda_i) \cdot p_a(\theta_v, \phi_v; \theta_o, \phi_o; \lambda_i)}{\omega_a(\lambda_j) \cdot \tau_a(\lambda_j) \cdot p_a(\theta_v, \phi_v; \theta_o, \phi_o; \lambda_j)}$$

The parameters $\tau_a(\lambda)$, $\omega_a(\lambda)$, and p_a are, respectively, the aerosol optical thickness, single-scattering albedo, and aerosol scattering phase function. Physically, $\varepsilon(\lambda_i, \lambda_j)$ represents the relative strengths of the aerosol scattering and absorption, largely independent of the power of the light incident upon the aerosol particles, viewing geometry, and the concentration of aerosol particles present.

For large, iron-rich, desert dust particles, the ratio of aerosol reflectances at 550 nm and 670 nm, $\varepsilon(550, 670)$, has been shown using CZCS data to decrease to 0.94 and below (Carder, Gregg et al. 1991) during strong dust events; typical values of 1.0-1.5 are found for smaller, nonabsorbing aerosols. In such occurrences, when aerosol reflectance is lower in the blue than the green or red, strong absorption is likely present.

Assuming complete avoidance of sun glitter, the total reflectance received at an ocean-viewing sensor can be described by:

$$\rho_t(\lambda) = \rho_r(\lambda) + \rho_a(\lambda) + \rho_{ra}(\lambda) + t(\lambda) \cdot [\rho_{wc}(\lambda) + \rho_w(\lambda)], \text{ where}$$

$$t(\lambda) = e^{-(\tau_R(\lambda)/2 + \tau_{O_3}(\lambda) + (1 - \omega_{\infty}(\lambda) \cdot F) \tau_{\infty}(\lambda)) / \cos\theta_o}$$

The subscripts represent the contributions from Rayleigh scattering, aerosol interactions (absorption *and* scattering), Rayleigh-aerosol interactions, whitecaps, and water-leaving radiance, respectively, and F the probability of forward scattering. Rayleigh scattering and whitecap reflectance may be determined *a priori* with knowledge of sun and spacecraft zenith angles and wind velocity. The diffuse transmittance of the atmosphere, $t(\lambda)$, is considered known since it is primarily a function of Rayleigh and ozone optical thickness (τ_r and τ_{O_3}) and the satellite zenith viewing angle, θ_v , and only secondarily a

function of aerosol attenuation (Gordon, Clark et al. 1983). Thus, separation of the total signal into components is reduced to that of determining the aerosol and water-leaving radiances.

Separation of $\rho_w(\lambda)$ and $\rho_{as}(\lambda)$ was effected for the CZCS using quasi-single scattering theory and clear-water radiances (Gordon, Clark et al. 1983). The basis for this theory is that where chlorophyll *a* plus pheophytin *a* concentrations are less than 0.25 mg m⁻³, the normalized water-leaving radiances, $L_{wn}(\lambda_i)$ can be designated *a priori* to within 10%. At 520, 550, and 670 nm these values are 0.495, 0.28, and less than 0.015 mW cm⁻² μm⁻¹ sr⁻¹, respectively. Thus, $\epsilon(520,670)$ and $\epsilon(550,670)$ were determined over clear water. For a given wavelength, $L_w(\lambda_i)$ can be related to $L_{wn}(\lambda_i)$ through

$$L_w(\lambda_i) = L_{wn}(\lambda_i)R(\theta_o, \lambda_i)\cos\theta_o$$

Clear-water radiances now determine $\rho_w(520)$, $\rho_w(550)$ and $\rho_w(670)$, yielding $\rho_{as}(\lambda)$ for these wavelengths at each pixel in a clear-water region (presumed to include most ocean regions away from land and within 35° latitude from the equator). Using the assumption that the aerosol size distribution behaves according to (Junge 1963) for the visible wavelengths,

$$\frac{dn(a)}{da} = C(z) \cdot a^\gamma,$$

where n is the aerosol particle number density, a the particle radius and γ the Junge parameter, the aerosol optical depth is given by (Van de Hulst 1957; Gregg and Carder 1990):

$$\tau_a(\lambda) = K \cdot \lambda^{-(\gamma+3)} = K \cdot \lambda^{-\eta_r(\lambda)}, \quad \eta_r = \gamma + 3 \text{ (Angström exponent)}$$

A further assumption of a single-scattering albedo of unity and non-spectral phase functions gives the aerosol epsilon:

$$\epsilon(\lambda_i, \lambda_j) = \frac{\rho_{as}(\lambda_i)}{\rho_{as}(\lambda_j)} = \left(\frac{\lambda_i}{\lambda_j} \right)^{-\eta_r(\lambda_i)}$$

AEROSOL ABSORPTION

Our initial investigations set aside direct measurements of particle concentration and size distributions and focus on observing the *in-situ* bulk absorption coefficient,

$$a(\lambda) = \frac{4\pi \cdot n_{IM}(\lambda)}{\lambda}$$

The optical properties of crustal aerosols have been extensively studied at source and island sites distant from the origin of aerosol dust types (Patterson and Gillette 1977; Patterson 1981) using diffuse reflectance techniques. The imaginary index of refraction, n_{IM} , increases significantly in the blue compared to the red and green wavelengths. The n_{IM} of Saharan dust, for example, was observed to increase log-linearly over the wavelengths 600 to 400 nm., approximately following

$$n_{IM}(400:600) \propto 10^{m\lambda}, \quad m \sim -3.6 \text{ such that}$$

$$a(\lambda) = \frac{4\pi \cdot 10^{-3.6\lambda}}{\lambda} \propto 10^{-(3.6\lambda + \log \lambda)}.$$

Rural dust samples from Texas, Denver and an Asian desert also exhibit monotonically decreasing absorption with increasing wavelength over these ranges.

RESULTS

Figure 1 is a SeaWiFS image of chlorophyll *a* concentration for the western Sargasso Sea on May 23, 1998, derived using Version 3.2 of Sea DAS processing code provided by the SeaWiFS Project of NASA. Note that instead of a typical homogeneous pattern with chlorophyll values from about 0.07 to 0.10 mg/m², extremely low values (0.01-0.06) are clustered near regions with high aerosol radiance (notice the box around low values).

Figure 2 is an image of the normalized water-leaving radiance at 555 nm, which should have a value near 0.27 mW/cm²/μm/sr. Notice the low values in the region where low chlorophyll values are found. Since the NASA chlorophyll algorithm (O'Reilly 1998) uses the ratio of normalized water-leaving radiance in Bands 3 and 5, a high ratio and low chlorophyll result from $L_{wn}(555)$ values below about 0.22 mW/cm²/μm/sr.

A question regarding the source of the error causing low $L_{wn}(555)$ and chlorophyll values is thus raised. Does it derive from poor calibration affecting the atmospheric correction, from a missing model for blue-absorbing desert dust in the atmospheric correction scheme, from the use of Band 7 in the atmospheric correction scheme with its inclusion of the oxygen-absorption line at 762 nm and inherent sensitivity to the height of the aerosol in the atmosphere, or from a combination of these?

To evaluate the aerosol-height question, the spatial co-variation between chlorophyll, $\epsilon(555,670)$, and an aerosol-height indicator were evaluated. To estimate the effects of aerosol height, a spectral-curvature algorithm (Campbell and Esaias 1983), $curv = L_r(750)^2/L_r(670)/L_r(865)$, was used. Here, values near 1.0 have no significant oxygen-absorption effects in the 750 nm band due to a negligible concentration of atmospheric gases being above the aerosol (e.g. cirrus clouds), while values well below 1.0 have increasingly more of an absorption effect due to a low effective height of the aerosols or clouds. In fact, the *curv* values for the rather uniform, unperturbed northern regions of the chlorophyll (Fig. 1) and the $L_{wn}(555)$ (Fig. 2) scenes were observed, *curv* values of 0.76 or less were observed. The aerosol models used in SeaDAS 3.2 were for boundary-layer aerosols, not dust, which were measured from 1.5 to 3.5 km altitude near Barbados (Talbot, Hariss et al. 1986) and were observed as a beige color and photographed from aircraft at 4 to 5 km on 19 May 1998 over the Bahamas, prior to these SeaWiFS observations. So high dust, high cirrus, and thin, wispy clouds all likely perturb Band 7 aerosol radiance retrievals such that an aerosol model is selected that is too blue in terms of its scattering characteristics. Excessive removal of aerosol radiance at 490 and 555 nm by SeaDAS 3.2 would increase the $\rho_w(490)/\rho_w(555)$ ratio for high-ratio waters and decrease it for low-ratio waters. For the Sargasso with the $\rho_w(490)/\rho_w(555)$ ratio typically > 3.0, high-altitude aerosols and thin clouds would increase the $\rho_w(490)/\rho_w(555)$ ratio and thus decrease retrieved values of chlorophyll.

Figure 3 is a composite of four image boxes from the low-chlorophyll area of Figure 1: a) $\epsilon(555,670)$ with values less than 0.97 masked in white; b) $curv > 0.76$ masked in white; c) $chl < 0.06$ masked in white; and d) $\epsilon(555,670) < 1.025$ masked in white. The low-epsilon pixels were clustered in the upper right part of the box, while the high-altitude aerosols occupied much of the rest of the box in almost a complementary fashion. In the lower part of the *curv* box are two triangular regions not explained by either the color or the height of the aerosols. If the epsilon mask is increased to 1.025, however, the combination of the area occupied by these aerosols and that by high-altitude aerosols coincide with most of the anomalous chlorophyll values.

One might expect to find only epsilon values smaller than 1.0 to be indicative of regions where absorbing aerosols would perturb the atmospheric correction procedure enough to affect chlorophyll retrieval accuracy. If, however, a higher-epsilon (e.g. 1.2), blue-scattering aerosol type is mixed with blue-absorbing dust, no evidence of blue absorption would be manifest at infrared wavelengths where the aerosol type is selected by the SeaWiFS algorithm. Thus, a higher-epsilon aerosol type would be selected in the infrared (e.g. 1.1) than is appropriate for atmospheric correction in the blue part of the spectrum if dust were present. Then significant perturbations to the chlorophyll field could still be occasioned by the presence of dust even without necessarily finding $\epsilon(555,670)$ values less than 1.0.

Another possible explanation for the co-variation of chlorophyll anomalies and regions where $\epsilon(555,670) < 1.025$ is calibration error. If Band 5 was high and Band 6 was low by 1% or so, then after correction for ρ_w and ρ_r , the $\epsilon(555,670)$ value 1.025 could be reduced to less than 1.0, and a much larger region would be identified as containing blue-absorbing aerosols. This possibility will be evaluated in the future.

CONCLUSIONS

We don't yet have a quantitative assessment of the exact combination of factors controlling the process producing $\rho_w(555)$ values that are unrealistically low for the scene studied in the Sargasso Sea. We do know the anomalous low-chlorophyll values are derived from the low $\rho_w(555)$ value, however. Certainly high-altitude clouds and aerosols produce $\rho_r(750)$ values that are higher than expected by the aerosol models used to correct for aerosol radiance in the SeaDAS 3.2 code, and the spectral curvature algorithm designated those areas with higher-altitude aerosols. These regions were always accompanied by lower-than-normal $\rho_w(555)$ and chlorophyll retrievals.

Regions, not affected by high clouds or aerosols but by aerosols with $\epsilon(555,670)$ values less than 0.97, were also found; these are presumed to contain iron-rich Saharan dust. These regions were always accompanied by lower-than-normal $\rho_w(555)$ and chlorophyll retrievals. An atmospheric-correction scheme independent of Band 7, using Bands 6 and 8 for aerosol typing over clear waters, is necessary to eliminate the aerosol-altitude effects of the oxygen-absorption band upon processing algorithms.

A final region was found with lower-than-normal $\rho_w(555)$ and chlorophyll retrievals, which were unexplained by the above arguments. This region did have values of $\epsilon(555,670) < 1.025$. We are not certain if values resulted from a mixture of blue-rich scattering, non-absorbing aerosols with blue-absorbing dust or if dust-rich pixels with

higher derived epsilon values are due to a calibration issue is not certain.

What is clear, however, is that anomalously low chlorophyll retrievals for the Sargasso Sea are not unusual, and a significant fraction of the pixels involved have an aerosol type found either higher in the atmosphere than expected by the atmospheric-correction scheme or have a red-rich $\epsilon(555,670)$. Further investigation of the calibration accuracy of Bands 5 and 6 is required in order to refine our interpretation of possible mixtures of aerosol types in the same air column.

REFERENCES

- Campbell, J. W. and W. E. Esaias (1983). "Basis for spectral curvature algorithms in remote sensing of chlorophyll." *Applied Optics* **22**(7): 1084-1093.
- Carder, K. L., et al. (1991). "Determination of Saharan dust radiance and chlorophyll from CZCS imagery." *J. Geophys. Res.* **99**(D3): 5369-5378.
- Carder, K. L., et al. (1991). "Reflectance model for quantifying chlorophyll a in the presence of productivity degradation products." *J. Geophys. Res.* **96**(C11): 20,599-20,611.
- Gordon, H. R., et al. (1988). "A semianalytical radiance model of ocean color." *J. Geophys. Res.* **93**(D9): 10,909-10,924.
- Gordon, H. R. and D. K. Clark (1981). "Clear water radiances for atmospheric correction of coastal zone color scanner imagery." *Applied Optics* **20**(24): 4175-4180.
- Gordon, H. R., et al. (1983). "Phytoplankton pigment concentrations in the Middle Atlantic Bight: comparison of ship determinations and CZCS estimates." *Applied Optics* **22**(1): 20-36.
- Gordon, H. R. and M. Wang (1994). "Retrieval of water-leaving radiance and aerosol optical thickness over the oceans with SeaWiFS." *Applied Optics* **33**(3): 443-452.
- Gregg, W. W. and K. L. Carder (1990). "A simple spectral solar irradiance model for cloudless maritime atmospheres." *Limnology and Oceanography* **35**(8): 1657-1675.
- Hurst, V. J. (1977). "Visual estimation of iron in saprolite." *Geological Society of America Bulletin* **88**: 174-176.
- Junge, C. (1963). *Air Chemistry and Radioactivity*, Academic Press.
- Lindberg, J. D. and L. S. Laude (1974). "Measurement of the absorption coefficient of atmospheric dust." *Applied Optics* **13**(8): 1923-1926.
- Martin, J. H., et al. (1994). "Testing the iron hypothesis in ecosystems of the equatorial Pacific Ocean." *Nature* **371**: 123-129.
- Martin, J. H. and S. E. Fitzwater (1988). "Iron deficiency limits phytoplankton growth in the north-east Pacific subarctic." *Nature* **331**: 341-343.
- Patterson, E. M. (1981). "Optical properties of the crustal aerosol: relation to chemical and physical characteristics." *J. Geophys. Res.* **86**(C4): 3236-3246.
- Patterson, E. M. and D. A. Gillette (1977). "Commonalities in measured size distribution for aerosols having a soil-derived component." *J. Geophys. Res.* **82**(15): 2074-2082.
- Schutz, L., et al. (1981). Saharan dust transport over the North Atlantic Ocean. *Desert Dust: Origin, Characteristics, and Effects on Man*. T. L. Pewe. Boulder, CO, Geological Society of America.
- Talbot, R. W., et al. (1986). "Distribution and geochemistry of aerosols in the tropical North Atlantic troposphere: relationship to Saharan dust." *J. Geophys. Res.* **91**: 5173-5182.
- Van de Hulst, H. C. (1957). *Light Scattering by Small Particles*. New York, John Wiley & Sons.
- Young, R. W., et al. (1991). "Atmospheric iron inputs and primary productivity: phytoplankton responses in the North Pacific." *Global Biogeochemical Cycles* **5**(2): 119-134.

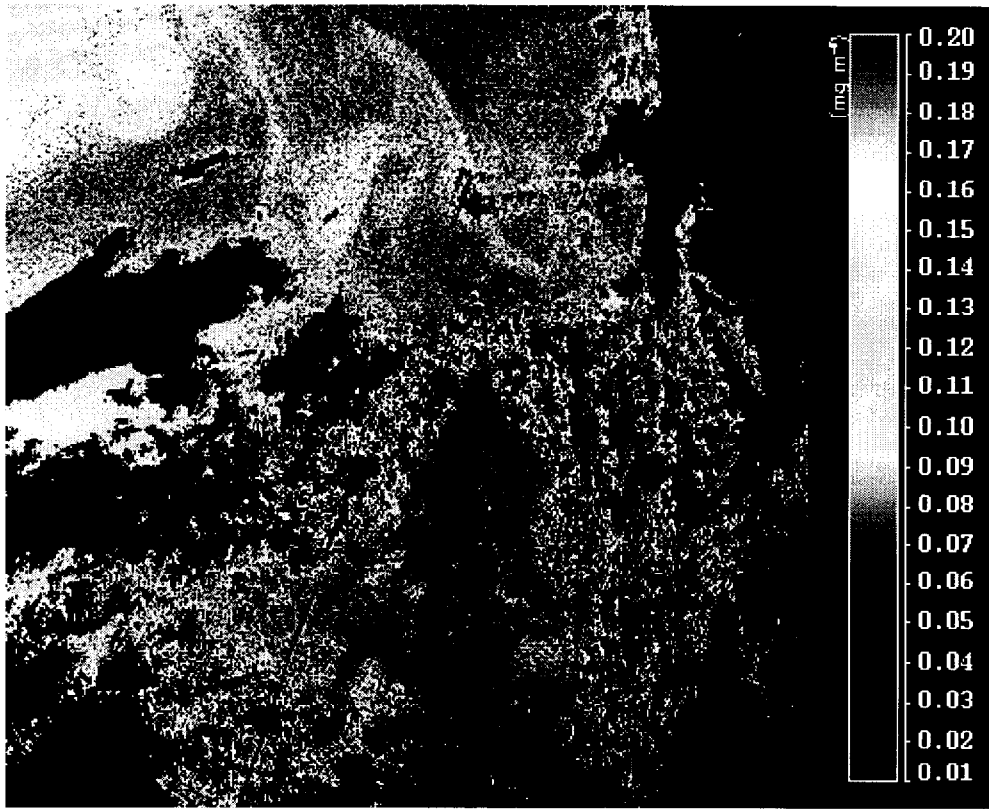


Figure 1. SeaWiFS image of chlorophyll a concentration for the western Sargasso Sea on May 23, 1998.

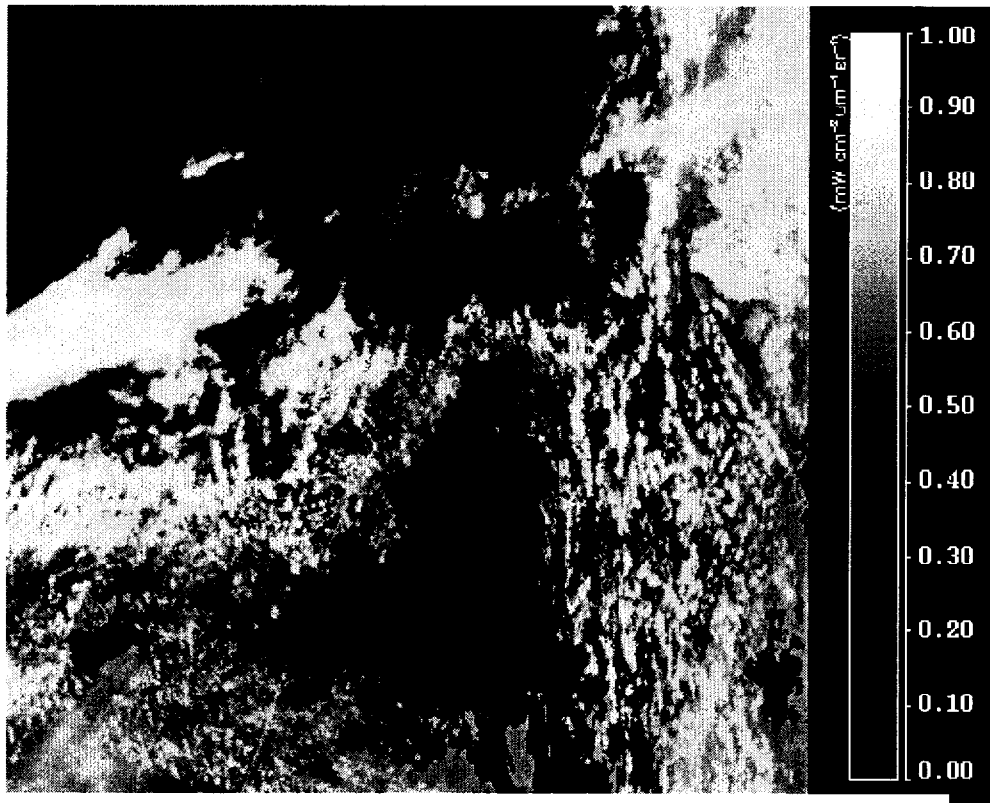


Figure 2. $L_{wn}(555)$ image as in Fig. 1.

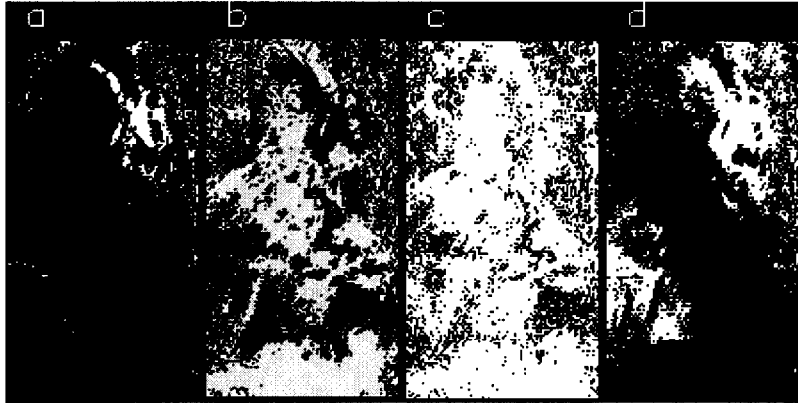


Figure 3. Data collected from the box in Fig.1: a) $\alpha(555,670)$ with values less than 0.97 masked in white; b) $curv > 0.76$ values masked in grey; c) $chl < 0.06$ values masked in white; d) $\alpha(555,670)$ values < 1.025 values masked in white.